https://doi.org/10.5194/egusphere-2026-482
Preprint. Discussion started: 3 March 2026

Comparison of M10 and M20 Meteomodem radiosondes relative humidity measurements with ECMWF ERA5 above France: focus on the upper troposphere.

Sidy Diarra[1,3], Nadège Montoux[1], Jean-Luc Baray[1,2], Philippe Keckhut[3], Jean-Charles Dupont[4], Antoine Farah[5], Dunya Alraddawi[3]

[1]LaMP, UMR6016, CNRS, Université Clermont Auvergne, Clermont-Ferrand, 63100, France

[2]OPGC, UAR833, CNRS, Université Clermont Auvergne, Clermont-Ferrand, 63100, France

[3]*LATMOS/IPSL, UVSQ Université Paris-Saclay, Sorbonne Université, CNRS, Guyancourt, France*

[4]Institut Pierre-Simon Laplace, École Polytechnique, UVSQ, Université Paris-Saclay, 92331 Palaiseau, France

[5]Meteomodem, 77300 Fontainebleau, France

Correspondence to : Nadège Montoux (nadege.montoux@uca.fr) and Sidy Diarra (sidy.diarra2@doctorant.uca.fr)

Abstract :

Accurate knowledge of the relative humidity (RH) in the troposphere is important for predicting cloud formation, particularly in the upper troposphere where contrails can form and contribute to global warming. However, it is difficult to predict their formation due to the lack of precise RH measurements at these altitudes. This paper compares RH data from Meteomodem radiosondes (M10 and M20) acquired over a 5-years period (2020-2024) at the Trappes and Nîmes meteorological stations in France with ECMWF ERA5 analyses, with a focus on the upper troposphere. For Trappes, two datasets exist: one processed operationally by Météo France (MF) and a second processed using the GRUAN standard. Whatever the processing is, Meteomodem radiosondes RH values are on average higher than ERA5 ones, by about 2 % at 800 hPa up to 10 % at 200 hPa. The operational MF processing generally gives higher RH than the GRUAN processing. The median difference between both processing methods is lower than 2.2 % for pressures higher than 300 hPa and is maximum for lower pressures and nighttime measurements, the GRUAN processing showing more consistency between daytime and nighttime measurements. The evolution of MF processing over time

https://doi.org/10.5194/egusphere-2026-482
Preprint. Discussion started: 3 March 2026

does not seem to affect the comparison. The major differences observed between the relative humidities measured by the sondes and those provided by the ERA5 reanalysis are between 200 and 300 hPa. First, ERA5 indicates more occurrences of RH below 40 % than the sondes. Second, the sondes indicate supersaturation conditions (~20 %) more frequently than ERA5 (11 %), probably due to the cloud parameterization in the IFS model, which fixes the RH at 100 % as soon as a cloud forms, in agreement to the higher occurrence of saturation conditions observed by ERA5 in this study. A first comparison of the results obtained at Trappes and Nîmes between the year 2020 and the years 2022, 2023 and 2024 shows no major differences, suggesting that the switch from M10 to M20 sondes in March 2021 at Nîmes does not significantly affect the ability to combine RH data for long term trends. However, more detailed investigations are required to assess finer differences. Finally, this study underlines the need to continue efforts to assess the quality of RH measurements in the upper troposphere and to improve cloud parameterizations in the model to increase supersaturation frequency in the upper troposphere as observed by the sondes.

Keywords : Relative humidity, radiosondes, ERA5, GRUAN, upper troposphere

https://doi.org/10.5194/egusphere-2026-482
Preprint. Discussion started: 3 March 2026

1. Introduction

Atmospheric water vapor plays a crucial role in the Earth's radiative balance, firstly because it is the main natural greenhouse gas, and secondly through the formation of clouds (Pruppacher and Klett, 1997), which themselves have an impact on the radiative balance (IPCC, 2013). The vertical distribution of water vapor in the troposphere is critical for mesoscale processes, particularly the development and persistence of convective systems (Sherwood et al., 2010). In addition to these natural processes, aviation also contributes to an additional Earth warming mainly due to the formation and persistence of contrails in the upper troposphere (Kärcher, 2018; Lee et al., 2021).

Calculating the relative humidity (RH) of the air mass allows to determine whether saturation is reached or not, a key factor in studying cloud formation and their radiative impact. However, RH depends both on the water vapour concentration and on the temperature. The accurate measurement of the water vapour concentration in the whole troposphere remains complex due to its rapid decrease with altitude, spanning several orders of magnitude, as well as its strong horizontal and temporal variability (Fischer et al., 2012; Konjari et al., 2025; Shao et al., 2023).

Satellite observations provide global coverage of RH. For example, Ruzmaikin et al. (2014) studied the tropospheric RH distribution and its influence on outgoing longwave radiation with the AIRS instrument. However these measurements have low spatial resolution and are in no way capable of reproducing the fine vertical structure of humidity observed in the tropopause region (Khaykin et al., 2009). On the other hand, measurements performed from commercial aircraft give RH in the upper troposphere but do not provide full coverage. One illustration is the MOZAIC (Measurement of ozone and water vapor by Airbus in-service aircraft) programme, which became IAGOS (In-service Aircraft for a Global Observing System) in 2011. (Smit et al., 2014) performed a reanalysis of upper troposphere humidity data from the MOZAIC programme for the period 1994 to 2009. Nevertheless, a dense measurement network is necessary for assimilation in numerical weather prediction models as studies have shown that disagreements between model and observations exist such as the difference in supersaturation occurrence between MOZAIC and ERA5 (ECMWF analysis) noticed by (Gierens et al., 2020) as well as RH biases between different models (Lang et al., 2021). Radiosondes,

https://doi.org/10.5194/egusphere-2026-482
Preprint. Discussion started: 3 March 2026

which cover altitude ranges from ground to the mid-stratosphere, can access these fine structures with in-situ sensors.

Many studies have characterized the RH distribution and trends using different types of radiosondes, the difficulty being to combine different instruments and technologies. For example, (Dai et al., 2011) have proposed statistical tests to detect changepoints to homogenize daily radiosonde humidity data and (McCarthy et al., 2009) have shown by combining multiple datasets that the extratropical Northern Hemisphere lower and mid-troposphere show moistening on the order of 1%–5 % per decade since 1970. In the past, radiosonde evaluations were conducted either by attaching multiple sondes to the same rig (Bock et al., 2013; Dirksen et al., 2024; Hoshino et al., 2022; Miloshevich et al., 2006) or by placing the sondes in a chamber simulating atmospheric descent (Miloshevich et al., 2001; Nash et al., 2010). These exercises allowed the development of a more homogeneous worldwide network with sondes from different manufacturers. At the same time, IGRA (Integrated Global Radiosonde Archive, (Durre et al., 2018)) was developed to provide data from more than 2800 stations around the world and GRUAN (GCOS Reference Upper-Air Network, (Seidel et al., 2009)) was created to provide climate-quality measurements of tropospheric and lower stratospheric variables such as water vapour.

Among the different radiosonde manufacturers, Meteomodem developed its first sonde, the GL98, in 1998, followed by the M2K2 in 2004. Since 2010, the M10 radiosonde has been used in more than 60 countries around the world, and since 2020, a more compact model, the M20, has been available. These radiosondes primarily rely on capacitive sensors consisting of a dielectric polymer placed between two electrodes, whose dielectric constant varies proportionally with RH.

To date, few studies have investigated the RH measurements provided by Meteomodem radiosondes in comparison with other data. For M10, Dupont et al. (2020) showed that radiosondes humidity measurements still face difficulties in covering the large dynamical range of water vapour, which spans several orders of magnitude and in performing measurements in mixed-phase conditions. Sondes also experience many spurious effects such as sensor response time and radiative effects. Dupont et al. (2020) applied the correction methods developed by Dirksen et al. (2014) for Vaisala RS92 sonde to M10 RH measurements

https://doi.org/10.5194/egusphere-2026-482
Preprint. Discussion started: 3 March 2026

at the Trappes site (France) in order to meet GRUAN standards. After correction, M10 measurements were on average consistent with those of the Vaisala RS92, with differences of 2 % RH at night (compared to 6 % before correction) and 5 % during the day compared to 9 % before correction) with M10 being more humid than Vaisala RS92.

The overall dry bias found by (Bock et al., 2013) for M10 radiosonde measurements relative to ground-based OHP lidar observations was likely related to the fact that these sondes belonged to the first production series. Concerning M20 sondes, they participated to the 2022 Upper-Air Instrument Intercomparison Campaign (Dirksen et al., 2024) which reported a wet bias of ~10 % relative to a Combined Working measurement Standard formed by RS41-SGP and iMS-100 radiosondes at around 10 km for nighttime measurements. They also concluded that the M20 sonde is capable of reporting 100 % RH inside clouds and does not overestimate ambient RH after exiting a cloud, a limitation that still affects other radiosondes types.

The aim of this study is to compare RH measurements from the M10 and M20 sondes with the ERA5 ECMWF reanalysis on the whole troposphere, taking into account that the RH can be calculated with respect to liquid water or to ice depending on the temperature as shown by (Song et al., 2020) over the Korean Peninsula with other sondes. For this purpose, radiosoundings conducted by Météo-France, the French meteorological operational center, at the Trappes station (48.77° N, 2.01° E) and the Nîmes station (43.87° N, 4.40° E) from 2020 to 2024 are used. In addition, M10 data recorded at the Trappes station has been reprocessed according to the GRUAN standards. These datasets allow a comparison of different processing methods and radiosonde types with ERA5 in the whole troposphere.

The details of the datasets and RH calculation are presented in Section 2, the results in Section 3, and the conclusions and perspectives in Section 4.

2. Data

2.1. ERA5 ECMWF reanalysis

ERA5 is the fifth-generation atmospheric reanalysis produced by the European Centre for Medium-Range Weather Forecasts (ECMWF). ERA5 data is generated using a numerical atmospheric model (Integrated Forecasting System) called IFS that provides detailed estimates of past and present atmospheric conditions across the entire globe. This model

https://doi.org/10.5194/egusphere-2026-482
Preprint. Discussion started: 3 March 2026

assimilates a wide range of real-time meteorological observations, including satellite, airborne, and terrestrial data such as radiosondes and dropsondes (Hersbach et al., 2020).

In this study, we extracted pressure, temperature, and specific humidity parameters at a horizontal resolution of 0.125 ° and a temporal resolution of one hour. To compare with radiosonde measurements which have a higher vertical sampling and could thus detect thinner atmospheric structures, we used the 137 native model levels rather than the interpolation on pressure levels to ensure maximum vertical resolution. This required recalculating RH (RH in percent) based on saturation vapor pressure (e_{sat} in Pascal) and specific humidity (q in kilogram of water vapor by kilogram of moist air), following the equation 1, which is derived from the IFS documentation. According to the temperature, the saturation vapor pressure is calculated following Equation 2:

- above liquid water ($e_{sat(w)}$) for temperature above 273.16 K according to Buck (1981) (Equation 3).
- above ice ($e_{sat(i)}$) for temperatures below 250.16 K according to Alduchov and Eskridge (1996) (Equation 4).
- or a combination of both for temperature between 250.16 K and 273.16 K (Equation 5).

$$RH = \frac{Pq\frac{1}{\epsilon}}{e_{sat}(1+q(\frac{1}{\epsilon}-1))} * 100 \quad \text{(Eq. 1)}$$

where ϵ is the ratio of the molar masses of water and dry air ($\epsilon = 0.621981$).

With :

$$e_{sat}(T) = \alpha e_{sat(w)}(T) + (1-\alpha)e_{sat(i)}(T) \quad \text{(Eq. 2)}$$

and

$$e_{sat(w)} = 611.21 * e^{(17.502(\frac{T-273.16}{T-32.19}))} \quad \text{(Eq. 3)}$$

$$e_{sat(i)} = 611.21 * e^{(22.587(\frac{T-273.16}{T+0.7}))} \quad \text{(Eq. 4)}$$

https://doi.org/10.5194/egusphere-2026-482
Preprint. Discussion started: 3 March 2026

$$\begin{cases} \alpha = 0 & T \leq 250.16\,K \\ \alpha = \left(\frac{T-250.16}{23}\right)^2 & 250.16 < T < 273.16\,K \\ \alpha = 1 & T \geq 273.16\,K \end{cases} \quad \text{(Eq. 5)}$$

During the study period, the humidity measurements from the radiosondes launched from Trappes were assimilated in ERA5 up to 100 hPa (Bell et al., 2021; Hersbach et al., 2020). This is not the case for the radiosondes launched from Nîmes.

2.2. Meteomodem radiosondes

The data used in this study was provided by the French meteorological operational center, Météo-France, which performs radiosounding measurements twice a day, once at night (~23:15 UTC) and once during the day (~11:15 UTC), from various locations in France using Meteomodem Automatic Radiosonde Launcher (ARL). Data was obtained during the ascent phase of the balloons, before their burst (on average at ~25 km). The maximum ascent duration of the balloons is 1 hour 45 minutes, with an average vertical sampling of 10 m (vertical ascent around +5 m s^{-1}), corresponding to approximately 2000 data points per sounding due to a measurement frequency of 1 Hz. For this study, we used data from the Nîmes and Trappes stations recorded from 2020 to 2024. M10 sondes were used throughout this period, except at Nîmes after March 2021, when M20 sondes were launched. Technical information of these two sondes is provided in the following subsections.

2.2.1 M10 type

The M10 radiosonde, marketed by the company Meteomodem since 2010, measures 95 mm x 95 mm x 88 mm and weighs 150 g (including batteries). It is equipped with a capacitive humidity sensor covered by an innovative metal shield. This shield ensures efficient ventilation while protecting the sensor from direct radiation and water droplet freezing. It also integrates a temperature sensor located at the end of the sensor probe and a GPS sensor. The GPS sensor provides the balloon's position from which pressure, vertical velocity, wind speed and direction can be derived.

The capacitive humidity sensor consists of three main elements: a base layer functioning as an electrode, a dielectric substance whose properties vary with humidity, and a porous, fast-response electrode serving as the second electrode of the capacitor. A secondary thermistor,

https://doi.org/10.5194/egusphere-2026-482
Preprint. Discussion started: 3 March 2026

positioned under a protective shield near the humidity sensor, provides a temperature measurement to calibrate the humidity retrieval. The precision given by the manufacturer is 3 % for RH in the 0 to 100 % range and 0.3 °C for temperatures in the -100 °C to +60 °C range.

The technology of Meteomodem radiosondes is now deployed in 60 countries. All new Meteomodem stations installed since 2011 use the M10 technology (Dupont et al., 2020). Since March 2021, some Météo-France stations, including Nîmes, have switched to the M20 type.

2.2.2 M20 type

The M20 radiosonde is an evolution of the M10 model. It is designed to be significantly lighter and more environmentally friendly, with dimensions of 98 mm × 63 mm × 42 mm for a total weight of 36 grams, including the battery. The M20 is equipped with a redesigned capacitive humidity sensor featuring an integrated heating system (which can be switched off) that activates when the sensor passes through clouds, minimizing condensation and frost formation, that can compromise measurement accuracy. A built-in barometer has been added, enabling more precise pressure measurements, especially in the lower atmosphere. The sensor response time is now less than 0.3 s at 1000 hPa and 20 °C, and around 50 s at 300 hPa and –55 °C. The M20 also offers environmental advantages using 15–30 % less launch gas, allowing for smaller balloons, and potentially eliminating the parachute while maintaining the same altitude performance.

2.2.3 RH calculation for Meteomodem radiosondes

The operational output product of radiosondes is the dew point temperature calculated from the Sonntag formulation (Sonntag, 1994). To compare with RH provided by ECMWF ERA5, conversions have to be performed. The formulas for these conversions are given as follows:

- We used the Sonntag formulation available between 173.15 K and 373.15 K to calculate the water vapor pressure with respect to water (e in hPa):

$$log(e) = \frac{-6096.9385}{T_e} + 16.635794 + -2.711193 \times 10^{-2} T_e + 1.673952 \times 10^{-5} {T_e}^2 + 2.433502\ log(T_e) \quad \text{(Eq.6)}$$

where T_e is the dew point temperature in Kelvin.

https://doi.org/10.5194/egusphere-2026-482
Preprint. Discussion started: 3 March 2026

- For the saturation vapor pressure, we used the ECMWF-ERA5 parameterization (Equations 2 to 5) with the temperature recorded by the sonde.
- Finally, the RH is calculated by Equation 7 :

$$RH = 100 \times \frac{e}{e_{sat}(T)} \quad \text{(Eq.7)}$$

The resulting RH depends on the temperature T: if T ≤ 250.16 K , it represents RH over ice ; if T ≥ 273.16 K, it represents RH over liquid water and if 250.16 < T < 273.16 K, it represents a mixed-phase RH.

2.3 The GRUAN Network

Météo-France radiosonde observations obtained with M10 sondes are operational measurements and datasets are primarily designed for short-term weather forecasting. To make this data suitable for scientific studies over both short and long timescales, it needs to be consolidated. This is one of the missions of the Global Climate Observing System (GCOS) Reference Upper Air Network (GRUAN, https://www.gruan.org/), an international initiative providing a reference-quality observing system, to address key gaps in the current global atmospheric monitoring network. GRUAN delivers long-term, high-precision observations extending from the surface through the troposphere and into the stratosphere, supporting the monitoring of climate trends, validation and calibration of satellite measurements, and improved understanding of atmospheric processes (Vömel et al., 2009).
M10 data from Trappes has been corrected according to Dupont et al. (2020) to be included in the GRUAN network and to align with GRUAN standards (Seidel et al., 2009). These adjustments addressed: (1) calibration biases; (2) the sensor's slow response, particularly under very high or very low RH conditions due to limited molecular diffusion; (3) the influence of temperature gradients on the humidity sensor measurements; and (4) the response delay at low temperatures, which can impact readings in areas with sharp humidity gradients. The GRUAN-corrected RH data set (Dupont et al., 2020) has been available since 2018. Data from Trappes has already been used for comparison with lidar observations acquired 20 km away at the SIRTA station (Alraddawi et al., 2025).

As with the M10 data from Météo-France, the M10 data from Trappes processed by GRUAN cannot be directly compared with ECMWF-ERA5, because RH is given with respect to liquid water (RH_w) using the Hyland and Wexler formulation (Hyland and Wexler, 1983), regardless

https://doi.org/10.5194/egusphere-2026-482
Preprint. Discussion started: 3 March 2026

of the water phase. To compare with the RH calculated from ERA5 data (section 2.1), conversions need to be performed. The formulas for these conversions are given as follows:

- We used the Hyland and Wexler formulation to calculate the saturation water vapor pressure with respect to liquid water (e_{satHW} in Pascal):

$$log(e_{satHW}) = \frac{-0.58002206\times10^4}{T} + 0.13914993 \times 10^1 - 0.48640239 \times 10^{-1}\mathrm{T} + 0.41764768 \times 10^{-4}\,\mathrm{T}^2 - 0.14452093 \times 10^{-7}\mathrm{T}^3 + 0.65459673 \times 10^1 log(\mathrm{T}) \quad \text{(Eq.8)}$$

where T is the temperature in Kelvin.

- The saturation vapor pressure e_{sat}, is estimated using the ECMWF-ERA5 parameterization (Equations 2 to 5) with the temperature recorded by the sonde.
- Finally, the RH is calculated by Equation 9:

$$\mathrm{RH} = \mathrm{RH}_w \times \frac{e_{satHW}}{e_{sat}} \quad \text{(Eq.9)}$$

As for M10 and M20, the resulting RH is over ice, liquid water or mixed-phase according to the temperature.

3. Daily and vertical variations of RH

3.1 Mean RH vertical profiles

A first objective of this study is to quantify the differences between the M10 data and the ERA5 reanalysis. For the M10 data, two processing methods are available : the GRUAN processing ($M10_{GRUAN}$) and the Météo France operational processing ($M10_{MF}$). This comparison is based on 1245 nighttime and 1249 daytime RH radiosounding profiles, acquired between 2020 and 2024 included from Trappes. For each radiosounding profile, a colocated ERA5 RH profile has been calculated by 3D interpolation in space of the ERA5 reanalysis at 12:00 PM for daytime profile or 12:00 AM for nighttime profile taking into account the sonde displacement. Then, to enable profile averaging, the data has been resampled by dividing the 900–100 hPa range into 10 hPa bins, within which the values have been averaged to get profiles with a 10 hPa vertical resolution. The same has been made for the ERA5 profile created. Finally, a mean profile as well as a 2-standard deviation profile have been calculated

https://doi.org/10.5194/egusphere-2026-482
Preprint. Discussion started: 3 March 2026

with the 1245 nighttime profiles at 10 hPa vertical resolution for $M10_{GRUAN}$, $M10_{MF}$ and ERA5. The same has been done with the 1249 daytime profiles at 10 hPa vertical resolution. Figure 1 presents the intercomparisons of mean RH profiles obtained from the two processing methods and from ECMWF ERA5, with the dataset separated into nighttime (a) and daytime (b) measurements.

The three datasets provide similar mean RH profile shapes, with a gradual decrease from ~76 % to ~47 % RH between 900 and 600 hPa (~1 to 4 km) followed by a gradual increase from ~47 % to ~70 % RH between 600 and 300 hPa (~4 to 9 km). Above this level, RH decreases sharply from ~70 % to ~10 % RH between 300 and 150 hPa (~9 to 12 km) and remains very low (a few percent) up to 100 hPa (~16 km). No strong discrepancies are observed in the shape of mean RH profiles during nighttime (Figure 1a) and daytime (Figure 1b). Tests have been performed using median of profiles (not shown) instead of mean of profiles and the shapes and magnitudes of the profiles are the same, meaning that no extreme values impact the comparison.

Between 900 hPa and 200 hPa, radiosondes ($M10_{MF}$ and $M10_{GRUAN}$) exhibit higher mean RH value than ERA5 despite their assimilation in the model. This difference, less than 2 % for pressures greater than 800 hPa (and within the measurement accuracy of the sondes), increases with altitude to reach around 8-9 % around 300 hPa. This result differs from the conclusion of Virman et al. (2021) which found ERA5 more humid than radiosondes measurements of 2-6 % at 650-800 hPa. This difference could be due to two factors:

1) The comparison was performed in a different environment: above the Tropical western Pacific Ocean during the convective period (November to February).
2) The comparison was performed with different sonde types from the Integrated Global Radiosonde Archive (IGRA) version 2.

For pressures lower than 200 hPa, $M10_{MF}$ mean RH values are systematically higher than those of ERA5, by ~5 % during daytime and ~10 % during nighttime, while $M10_{GRUAN}$ is in better agreement with ERA5. The difference between the two M10 processings is greater for nighttime measurements than for daytime measurements with differences between 300 and 900 hPa which could reach 5 % at 300 hPa for nighttime measurements.

https://doi.org/10.5194/egusphere-2026-482
Preprint. Discussion started: 3 March 2026

The dotted lines in Figure 1 indicate the 2-standard deviation, which gives an indication of the RH variability according to the altitude. For the three datasets, the 2-standard deviation is quite constant between 800 and 200 hPa around 12-13 % and one quarter lower at 900 hPa. For pressure lower than 200 hPa, the 2-standard deviation decreases down to a few percent. ERA5 has the lowest variability, followed by $M10_{MF}$ and then by $M10_{GRUAN}$.

The main difference between ERA5 and radiosondes mean RH vertical profiles is observed around 300 hPa (~9 km), an altitude where accurate measurements are necessary for studying cirrus clouds and contrails formation. This observation was previously reported by Alraddawi et al. (2025) which used $M10_{GRUAN}$, ERA5 and ground based IPRAL lidar data to conclude that ERA5 systematically underestimates water vapour at cruise altitudes, with a dry bias increasing from 10 % at 9 km to >20 % at 11 km. In the following section, we investigate the origin of this difference.

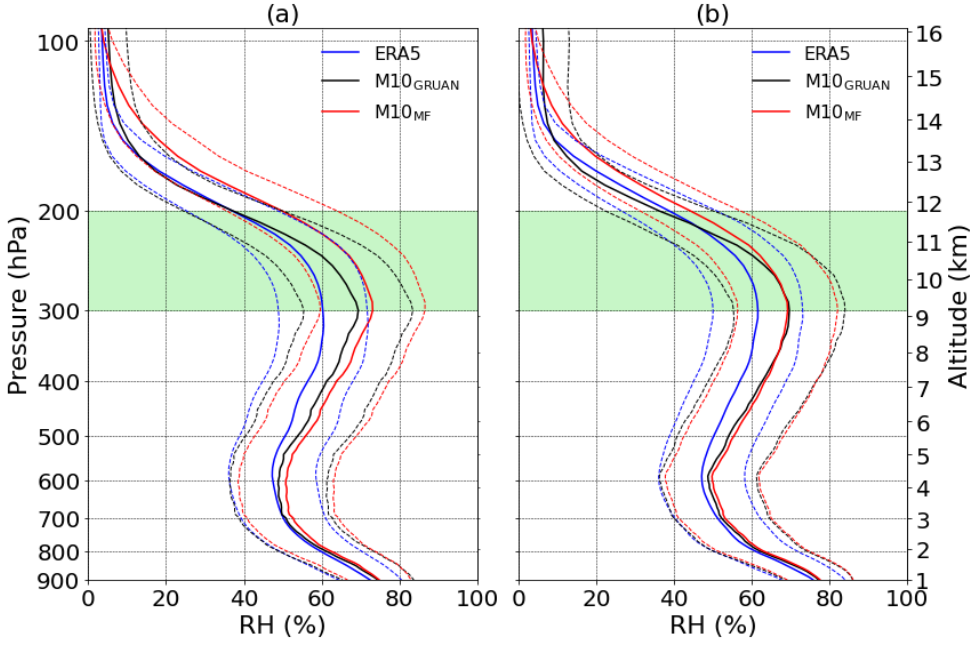

Figure 1. ERA5 (blue), $M10_{GRUAN}$ (black) and $M10_{MF}$ (red) mean RH vertical profiles over Trappes during five successive years (from 2020 to 2024), during night (a) and day (b). The dotted lines indicate the 2 standard deviation range, while the light green shaded band between 200–300 hPa represents the typical contrail formation altitudes.

https://doi.org/10.5194/egusphere-2026-482
Preprint. Discussion started: 3 March 2026

3.2 Focus on the 200–300 hPa layer (~9 to 12 km altitude)

To compare the distributions of radiosonde observations ($M10_{GRUAN}$ and $M10_{MF}$) and ERA5 outputs in the 200–300 hPa layer, we extracted all data points from the native resolution profiles available over the 5 years period where pressure values are between 200 hPa and 300 hPa and aggregated them to produce histograms with 5 % RH bin range (Figure 2).

The water vapor distribution in the upper troposphere (300–200 hPa, ~9 to 12 km altitude) reveals distinct shapes between ERA5 and radiosonde observations from both processing methods ($M10_{GRUAN}$ Figure 2a and $M10_{MF}$ Figure 2b). ERA5 RH distribution is quite flat (or slightly decreasing) from 0 to 95 % with an average occurrence of 4.4 % per 5 % RH bin range except for one peak between 5 and 10 % of RH reaching 7.0 % of occurrence. Above 95 % of RH, occurrences near saturation (95–105 %) are high (12.1 %), supersaturation occurrences are lower and decrease as RH increases, with no values above 165.9 %.

The radiosondes ($M10_{GRUAN}$ and $M10_{MF}$) present fewer occurrences of RH below 40 % compared to ERA5, except for RH values lower than 5 %, where $M10_{GRUAN}$ shows a peak frequency of 11.2 %, more than twice that of ERA5. This peak is due to the occurrence of a large number of 0 in the RH values (6.95 %). Between 40 and 95 %, $M10_{MF}$ and ERA5 are in good agreement with similar occurrences, while $M10_{GRUAN}$ shows slightly lower occurrences. The peak observed around the saturation by ERA5 is not observed by the radiosondes; however, the radiosondes show higher frequency of supersaturation : 19.5 % for $M10_{GRUAN}$ and 21.1 % for $M10_{MF}$ compared to 11.3 % for ERA5. The operational processing retrieves higher supersaturation compared to the GRUAN processing: up to 189.2 % for $M10_{GRUAN}$ and up to 192.5 % for $M10_{MF}$. Despite the assimilation of the $M10_{MF}$ by the IFS model to produce ERA5, the two RH distributions diverge, particularly for RH <40 % and RH >90 %.

Hofer et al. (2024) studied the possibility to predict ice-supersaturated regions where contrails can persist. They compared cumulative RH above ice distributions from MOZAIC/IAGOS data (16 588 flights over 10 years at midlatitudes, 310–190 hPa) with the corresponding ERA5 distributions. They also found that the two distributions differ, particularly near saturation.

https://doi.org/10.5194/egusphere-2026-482
Preprint. Discussion started: 3 March 2026

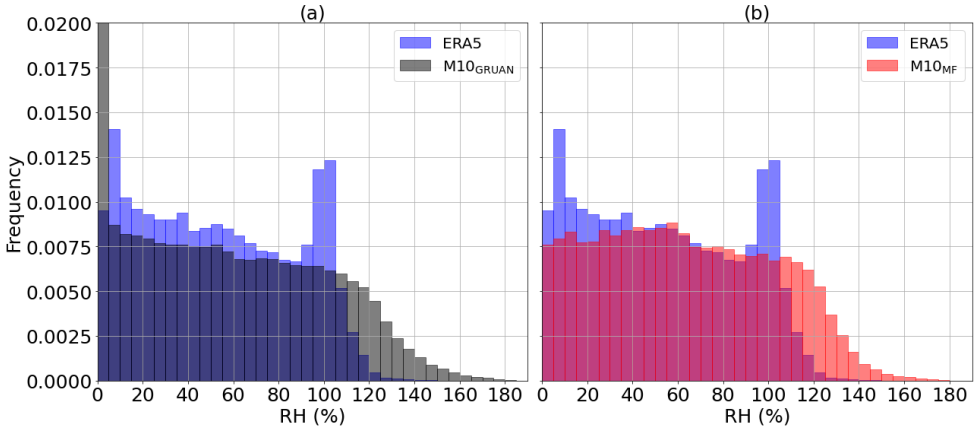

Figure 2. RH frequency histograms for (a) ERA5 (blue) and $M10_{GRUAN}$ radiosondes (grey) and (b) ERA5 (blue) and $M10_{MF}$ radiosondes (orange) over a five-year period (2020 - 2024) in the 200–300 hPa range.

The comparison of histograms alone does not provide sufficient evidence to determine whether the RH peak observed between 90 % and 105 % by ERA5 corresponds to situations where radiosondes detect supersaturation. To address this question, we applied the following procedure :

1) Each ERA5 and M10 profile was interpolated at the vertical resolution of the M10 radiosounding performed on 1 January 2020.
2) At each altitude, ERA5 values from all profiles were divided into two groups: those with RH above 90 % and their corresponding M10 points (labeled RH > 90 %) and those with RH below 90 % and their corresponding M10 points (labeled RH < 90 %). This yields two series of data pairs.
3) For each pair, the RH difference ΔRH = M10 - ERA5 was calculated at each altitude.

The vertical profiles, presented in Figure 3, are the median, the 5th and 95th percentiles of the RH differences between radiosondes and ERA5, calculated at each altitude for each series.

Under dry conditions (RH < 90 %), which represent more than 1695 of the 2494 profiles available at each level (Figure 3c), the median RH differences between radiosondes and ERA5 remain relatively small, less than 5 % on average, indicating quite good agreement in the 300 to 200 hPa layer (~9 to 12 km altitude) over the five-year period. The median RH differences

https://doi.org/10.5194/egusphere-2026-482
Preprint. Discussion started: 3 March 2026

are negative for the GRUAN processing (ERA5 RH higher than $M10_{GRUAN}$ RH) and positive for the Météo-France processing (ERA5 RH lower than $M10_{MF}$ RH). According to the 5th and 95th percentiles, RH differences can reach -33.5 % to +29.2 % for the GRUAN processing and -28.7 % to +34.8 % for the MF processing.

In contrast, under wet conditions (RH > 90 %), which represent less than 800 profiles of the 2494 profiles available at each level in the 200-300 hPa layer, discrepancies increase markedly. ΔRH medians range between 21.6 % and 27.5 % for both $M10_{GRUAN}$ and $M10_{MF}$ indicating that radiosondes often exhibit higher RH than ERA5 under moist conditions. However, this is not always the case, as the 5th percentile is negative, reaching -14 %. The variability of ΔRH in wet conditions is smaller than in dry conditions and is also not symmetric, with medians closer to the 95th percentile than the 5th percentile.

These results show that ERA5 tends to underestimate supersaturation events that are often recorded by radiosondes. This may be related to the cloud parameterization in the IFS model, which could trigger cloud formation too quickly, leading to an instantaneous reduction of water vapour to the saturation level upon nucleation (Tompkins et al., 2007).

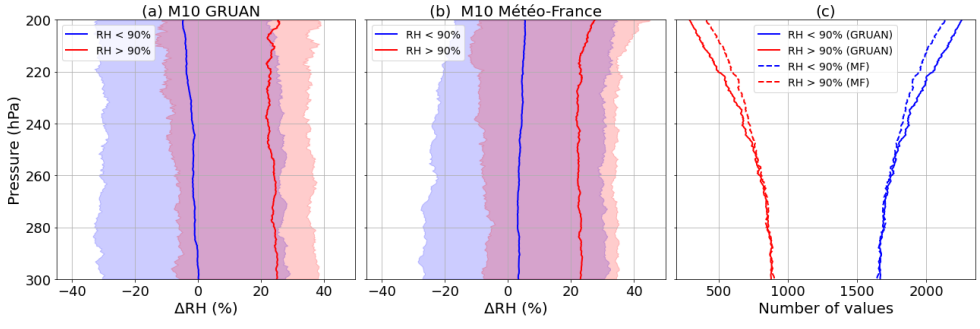

Figure 3. Vertical profiles of differences between (a) $M10_{GRUAN}$ and ERA5 (b) $M10_{MF}$ and ERA5 according to humidity conditions : RH ERA5 < 90 % in blue or RH ERA5 > 90 % in red over five years of observations (from 2020 to 2024) in the 200 hPa - 300 hPa range. The solid lines are the medians of the RH differences, and the shaded areas indicate the 5 and 95 percentiles range. (c) Corresponding number of values used for each condition, GRUAN (solid lines) and Météo-France (dashed lines).

https://doi.org/10.5194/egusphere-2026-482
Preprint. Discussion started: 3 March 2026

3.3. Impact of the data processing evolution on the RH measurements

On Figure 3, a difference in RH is observed between the GRUAN processing and the Météo-France processing. This part will focus deeply on the difference observed between the two processings across the time. Indeed, while the GRUAN processing is a reprocessing of the M10 radiosounding data according to Dupont et al. (2020) and is thus stable with time, the Météo-France processing evolves across the time as changes of the retrieval are regularly done by Meteomodem, so it is necessary to follow the difference between the two processings with time.

For each radiosonde recorded at the Trappes station between 2020 and 2024, the RH difference between the Météo-France processing ($M10_{MF}$) and the GRUAN processing ($M10_{GRUAN}$) was calculated. This comparison is based on 436 profiles in 2020, 613 profiles in 2021, 474 profiles in 2022, 516 profiles in 2023 and 455 profiles in 2024 mixing daytime and nighttime profiles. Then minimum, quartiles and maximum of RH differences were calculated by bins of 50 hPa from 900 hPa to 100 hPa for each year and for the entire period. The resulting statistics are displayed in Figure 4 as boxplots for the full period, while the yearly evolution of these parameters is shown in Table 1 for two pressure layers: 900-400 hPa and 300-200 hPa.

https://doi.org/10.5194/egusphere-2026-482
Preprint. Discussion started: 3 March 2026

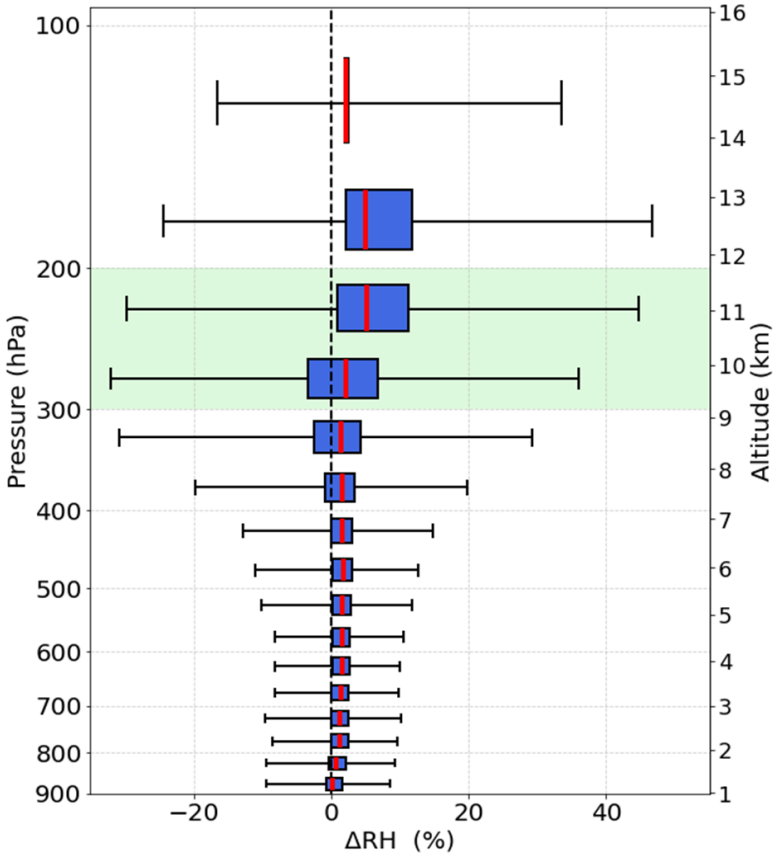

Figure 4. Boxplots of RH differences between M10 Météo-France processing ($M10_{MF}$) and M10 GRUAN processing ($M10_{GRUAN}$) *for radiosoundings at the Trappes site from 2020 to 2024.*

Overall, the comparison shows a very good agreement between the two processing methods from 900 hPa (≈1 km) to 300 hPa (≈9 km), with median differences remaining below 2.2 %, within the 3 % precision specified by the manufacturer. On average, $M10_{MF}$ relative humidities are 1.2 to 1.8 % higher than those from $M10_{GRUAN}$ in this pressure range. From 900 hPa to 500 hPa, RH difference between the two processings can reach 14.8 % as shown by the minimum and maximum of the boxplots. From 500 hPa to 200 hPa, the minimum and maximum differences in RH increase, with extreme values reaching -32.1 % for the minimum difference (between 250 and 300 hPa) and 44.8 % for the maximum difference (between 200 and 350 hPa). They decrease then in the range 200 to 100 hPa. The mean difference is maximum in the range 200 to 250 hPa and reaches 5.2 %.

https://doi.org/10.5194/egusphere-2026-482
Preprint. Discussion started: 3 March 2026

Table 1: Annual values of RH differences between M10 Météo-France processing ($M10_{MF}$) and M10 GRUAN processing ($M10_{GRUAN}$) at Trappes from 2020 to 2024. Values are shown for two pressure layers (900–400 hPa and 300–200 hPa). Columns indicate the minimum (Min), first quartile (Q25), median (Q50), third quartile (Q75) and maximum (Max) of RH differences for each year.

Pressure layer	300–200 hPa					900–400 hPa				
Year	Min (%)	Q25 (%)	Q50 (%)	Q75 (%)	Max (%)	Min (%)	Q25 (%)	Q50 (%)	Q75 (%)	Max (%)
2020	-28.7	-2.3	3.3	8.7	41.2	-8.4	-0.3	1.3	2.6	10.8
2021	-32.1	-1.8	4.7	11.3	44.8	-12.9	-1.0	1.2	2.9	14.8
2022	-23.3	-1.1	3.7	8.8	38.1	-5.4	0.6	1.8	2.8	9.2
2023	-18.1	0.8	4.5	9.3	36.4	-6.1	0.1	1.3	2.4	9.4
2024	-25.5	-2.7	2.5	7.1	29.1	-5.8	<0.1	1.2	2.2	8.3

According to Table 1, no systematic trend is apparent over the five-year period in the two pressure layers, with median differences remaining consistently below 5 % across all years. The largest differences between the two processing methods are observed in 2021, which also has the highest number of profiles available for comparison. A decrease in maximum differences is observed in the 300-200 hPa layer after 2021 (from approximately 45 % to 29 %). However, additional years would need to be analyzed to account for interannual variability and to determine whether this change reflects an evolution of the processing software.

3.4. Impact of radiosondes type on RH measurements

From March 2021, the Nîmes station switched from M10 to M20 radiosondes, while Trappes continued operating M10 radiosondes. This configuration provides an opportunity to evaluate whether the transition between sonde generations introduced any discontinuity or systematic change in RH measurements, by comparing the RH differences of M10 and M20 relative to ECMWF ERA5 data.

To this end, four years of data were analyzed:

- 2020, when only M10 ($M10_{MF}$) sondes were deployed at both Nîmes and Trappes,

https://doi.org/10.5194/egusphere-2026-482
Preprint. Discussion started: 3 March 2026

- 2022, 2023 and 2024, when M20 ($M20_{MF}$) sondes were in operation at Nîmes, while Trappes continued with M10 ($M10_{MF}$) sondes.

The year 2021 has been omitted because the switch from M10 to M20 sondes occurred in March at Nîmes. Since the number of radiosoundings per year was much higher at Nîmes than at Trappes, only the dates when measurements were available at both stations were retained, ensuring a similar monthly distribution for each station. The number of selected profiles for each year is listed in Table 2.

Table 2: Number of daytime and nighttime profiles selected for each year for both the Nîmes and Trappes stations.

Year	Daytime	Nighttime
2020	191	186
2022	208	204
2023	301	255
2024	224	231

Comparison of the monthly distribution of profiles (not shown) show nearly identical distributions for 2023 and, to a lesser extent, for 2024. However, in 2020 and 2022, fewer radiosoundings were available from August to December (43 and 74 profiles in 2020 and 2022, respectively, compared to 241 and 203 profiles in 2023 and 2024). This difference in monthly coverage could influence the calculation of annual variability.

Radiosonde data was systematically compared to collocated ERA5 profiles, used as a common reference, to determine whether the change in sonde type affects RH measurements. For each radiosounding, a colocated ERA5 RH profile was generated by 3D spatial interpolation of the ERA5 reanalysis at 12:00 UTC for daytime profile and 0:00 UTC for nighttime profile. All the radiosounding profiles and their corresponding ERA5 profiles were then interpolated onto the vertical sampling of the first radiosounding of 2020 to calculate the difference between both. Then, quartiles of the differences were calculated for each year, station and processing method, and are presented in Figure 5 for nighttime and daytime measurements separately.

https://doi.org/10.5194/egusphere-2026-482
Preprint. Discussion started: 3 March 2026

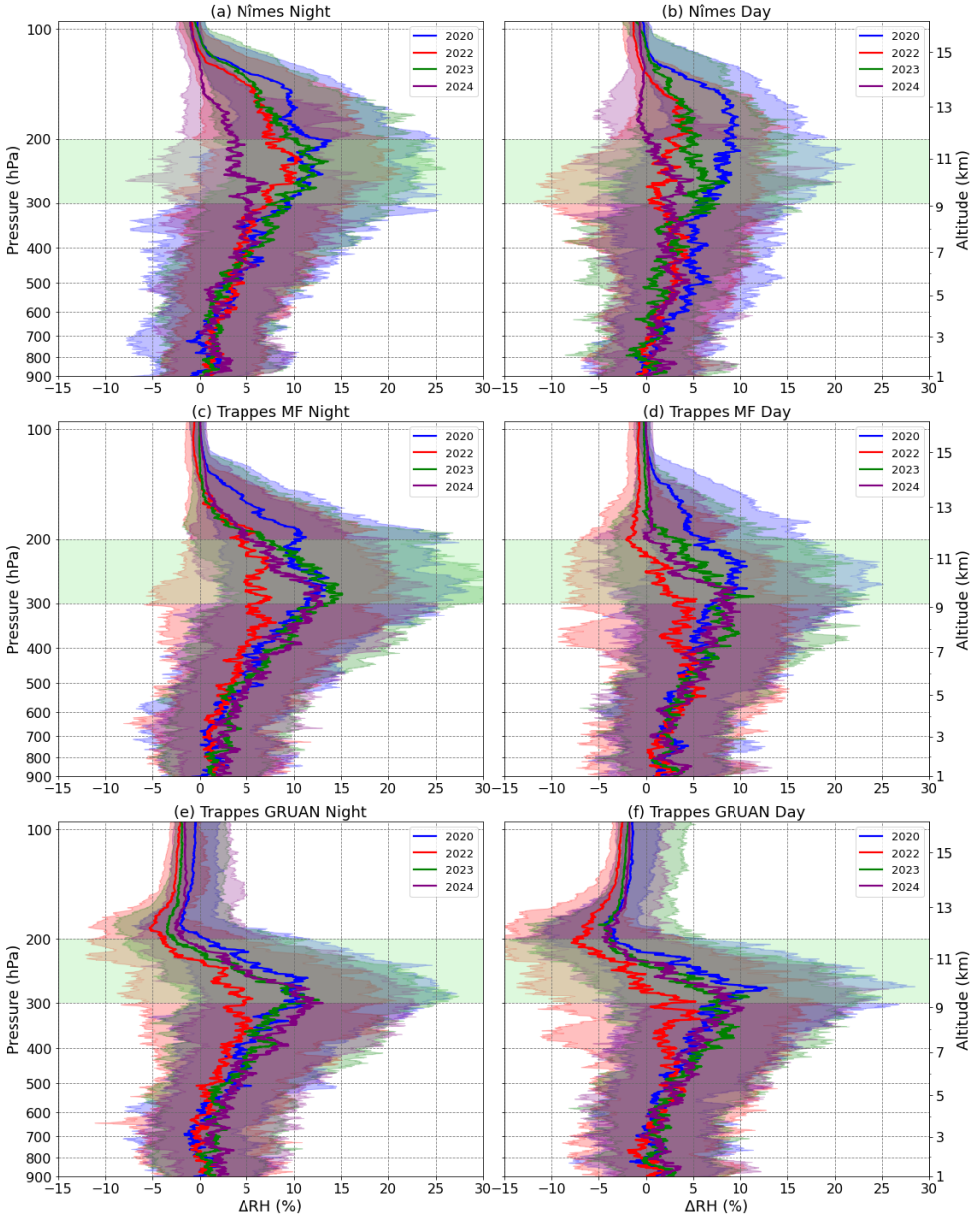

Figure 5. *Quartiles of the RH differences between Meteomodem sondes (M10 or M20) and ERA5* from 2020 to 2024 *: the shaded areas represent the 25-75 % interquartile range, while the solid lines represent the medians. Blue is for the year 2020, red for the year 2022, green for the year 2023 and purple for the year 2024. The left column (a, c and e) are for nighttime radiosoundings and the right column (b,d and f) are for nighttime radiosoundings. Top figures*

https://doi.org/10.5194/egusphere-2026-482
Preprint. Discussion started: 3 March 2026

(a and b) are for Météo-France processing at *Nîmes, middle figures (c and d) are for* Météo-France processing at *Trappes and bottom figures (e and f) are for* GRUAN processing at *Trappes.*

Before addressing the issue of radiosonde transition, we note that Figure 5 confirms the observations made in Figure 1 for the entire period 2020-2024 : radiosondes generally measure relative humidities higher than those provided by ERA5, especially between 200 and 300 hPa (~10 % RH difference). Between approximately 150 and 400 hPa, the differences between Météo-France and ERA5 processings are larger for nighttime measurements (Figures 5a and 5c) than for daytime measurements (Figures 5b and 5d) with a maximum difference of about 5 %. Although radiosonde data from Nîmes station is not assimilated into the IFS model producing ERA5 reanalysis, unlike Trappes, the observed differences between radiosonde and ERA5 RH are similar at both stations with the Météo-France processing.

For the Nîmes station, the median RH differences between radiosondes and ERA5 are larger in 2020 when M10 sondes were used, than in subsequent years with M20 sondes. However, the same pattern is observed at the Trappes station, which used M10 sondes throughout the period. This suggests that the larger difference observed at Nîmes in 2020 is more likely due to interannual variability than to the change in sonde type. The interannual variations observed in the median RH differences profiles (radiosonde - ERA5) do not appear to result from difference in sampling, as 2020 and 2022, years with fewer profiles from August to December, do not show similar profiles and are not substantially different from those of 2023 and 2024. Despite the sonde change, the greater RH difference observed at night compared to daytime persists at Nîmes in 2022, 2023 and 2024. As this daytime/nighttime difference is not visible for the GRUAN processing (Figures 5e and 5f), it seems that this difference could be reduced by processing improvements.

4. Conclusion

Five years (2020 to 2024) of Meteomodem radiosondes relative humidity (RH) measurements from the Trappes and Nîmes meteorological stations in France were compared to RH from the ECMWF ERA5 reanalysis. Differences between the operational Météo France processing ($M10_{MF}$) and the standardized GRUAN processing ($M10_{GRUAN}$) to retrieve RH from M10

https://doi.org/10.5194/egusphere-2026-482
Preprint. Discussion started: 3 March 2026

radiosondes measurements were evaluated. The impact of the switch from M10 to M20 sondes at the Nîmes station in March 2021 was also investigated.

Meteomodem radiosondes generally report higher RH values than ERA5, with differences increasing from 2 % at 800 hPa to 10 % at 200 hPa (Figure 1) for both processings. The two processings applied to the M10 measurements at Trappes are in good agreement between 900 and 300 hPa with median differences lower than 2.2 % indicating higher relative humidities in average for MF compared to GRUAN even if individual differences could reach ±30 % (Figure 4). The agreement is better for daytime measurements than for nighttime measurements, where the mean absolute difference reaches 5 % at 300 hPa (Figure 1). The difference between the two processings is maximum between 200 and 250 hPa (~11 km), with a median of 5.2 % (Figure 4). For the GRUAN processing, the RH difference observed between the radiosondes and ERA5 is similar during nighttime and daytime measurements while it is greater for nighttime measurements compared to daytime measurements for the MF processing (Figure 5). As the MF processing evolves with time by the modifications of the retrieval regularly pushed by Meteomodem, we would expect a better agreement with time between GRUAN and MF RH. However it is not the case as the major difference between MF and GRUAN occurs in 2021. The evolution of the MF processing with time seems thus not noticeable on the data. For pressure higher than 200 hPa, ERA5, $M10_{MF}$ and $M10_{GRUIAN}$ show similar RH variability which is not the case above where ERA5 shows the lowest variability and $M10_{GRUIAN}$ the highest one.

Between 200 and 300 hPa, ERA5 indicates more occurrence of RH lower than 40 % than sondes except close to 0 where ~7 % of relative humidities equal to 0 % are retrieved by the GRUAN processing (Figure 2). For higher RH values, ERA5 indicates more occurrence of conditions near the saturation (~12,1 % between 95 and 105 %) compared to the sondes while the sondes measure more occurrence of supersaturation conditions (~19,5 % for GRUAN and ~21,6 % for MF) compared to ERA5 (~11,2 %) as already mentioned in Hofer et al. (2024).

The maximum of supersaturation retrieved by the GRUAN processing (189.2 %) is lower than those retrieved by the MF processing (192.5 %). When ERA5 indicates relative humidities above 90 %, the difference between the sondes and ERA5 is much greater than when ERA5 relative humidities are below 90 % (Figure 3), which could be due to the cloud

https://doi.org/10.5194/egusphere-2026-482
Preprint. Discussion started: 3 March 2026

parameterization in the ISF model, which produces clouds too quickly and reduces the amount of water vapour to saturation level instantaneously during nucleation.

The lower agreement observed between sondes and ERA5 at Nîmes in 2020 compared to the more recent years doesn't seem to be due to the switch from M10 to M20 sondes as the same conclusion is observed at Trappes which didn't switch its sondes (Figure 5).

Altogether, these results seem to indicate that the modifications of the retrieval regularly implemented by Meteomodem to process radiosonde data, and the switch from M10 to M20 sondes do not have a statistically significant impact on RH estimates and thus shouldn't prevent climatological studies, although this should be confirmed with additional data in the future. The larger RH differences between sondes and ERA5 observed at night, mainly between 200 and 300 hPa, appears reducible through processing improvements, as they are only observed in the MF processing and not in the GRUAN processing.

The largest discrepancies between radiosondes and ERA5 RH occur between 200 and 300 hPa, the altitude range where cirrus and contrails form. As numerous studies are ongoing to try to reduce the non-CO_2 effect of aviation on climate warming, this study underlines the need to continue efforts to qualify the quality of RH measurements at these altitudes. To this end, a measurement campaign was carried out at the SIRTA station in May 2025 to provide RH measurements from different instruments launched on the same balloon (M10, M20 Meteomodem and Vaisala RS41 sondes). This could enable us to study the difference in supersaturation observed by the different probes in the same air masses, and to gain a better understanding of the limitations of each type of sonde, but also help to see how the different datasets can be combined to study long-term trends. Simultaneously, improvements of cloud parameterizations in models are underway. For example, the new ice-cloud scheme proposed by Sperber and Gierens (2023) seems promising but still requires further testing in more realistic situations before being implemented in models such as ISF. This type of scheme will enable us to see whether supersaturation is as frequent at this altitude as the probes observe.

https://doi.org/10.5194/egusphere-2026-482
Preprint. Discussion started: 3 March 2026

Code and data availability

The datasets and codes used in this study are available under https://doi.org/10.25519/he28-c712.

Author contribution

PK provided the funding and resources and designed the project. PK, NM, JLB designed the methodology. AF, JCD and DA provided information about datasets. SD analyzed the data. SD and NM wrote the manuscript draft. NM, JLB, PK, SD, JCD, DA and AF reviewed and edited the manuscript.

Competing interests

Author Antoine Farah is employed by the Meteomodem company.

Acknowledgments

The BECOM project has received funding from the Horizon Europe research and innovation actions program under grant agreement 101056885. CO-PDD is an instrumented site of OPGC observatory and LaMP laboratory, supported by Université Clermont Auvergne (UCA), Centre National de la Recherche Scientifique (CNRS-INSU) and Centre National d'Etudes Spatiales (CNES). We acknowledge Météo-France for the radiosonde data public availability (https://donneespubliques.meteofrance.fr). The ERA5 reanalysis data used in this study were provided by ECMWF (DOI:10.24381/cds.143582cf) and generated using Copernicus Climate Change Service information (C3S). The Authors would like to gratefully acknowledge the Meso-Center for ensuring access to and availability of the GRUAN data employed in this work (https://mesocentre.ipsl.fr/account-opening/).

References

Alduchov, O. A. and Eskridge, R. E.: Improved Magnus Form Approximation of Saturation Vapor Pressure, J. Appl. Meteorol., 35, 601–609, https://doi.org/10.1175/1520-0450(1996)035<0601:IMFAOS>2.0.CO;2, 1996.

Alraddawi, D., Keckhut, P., Mandija, F., Sarkissian, A., Pietras, C., Dupont, J.-C., Farah, A., Hauchecorne, A., and Porteneuve, J.: Calibration of Upper Air Water Vapour Profiles Using the IPRAL Raman Lidar and ERA5 Model Results and Comparison to GRUAN Radiosonde Observations, Atmosphere, 16, 351, https://doi.org/10.3390/atmos16030351, 2025.

https://doi.org/10.5194/egusphere-2026-482
Preprint. Discussion started: 3 March 2026

583 Bell, B., Hersbach, H., Simmons, A., Berrisford, P., Dahlgren, P., Horányi, A., Muñoz-Sabater, J.,
584 Nicolas, J., Radu, R., Schepers, D., Soci, C., Villaume, S., Bidlot, J., Haimberger, L., Woollen, J.,
585 Buontempo, C., and Thépaut, J.: The ERA5 global reanalysis: Preliminary extension to 1950, Q.
586 J. R. Meteorol. Soc., 147, 4186–4227, https://doi.org/10.1002/qj.4174, 2021.

587 Bock, O., Bosser, P., Bourcy, T., David, L., Goutail, F., Hoareau, C., Keckhut, P., Legain, D.,
588 Pazmino, A., Pelon, J., Pipis, K., Poujol, G., Sarkissian, A., Thom, C., Tournois, G., and Tzanos,
589 D.: Accuracy assessment of water vapour measurements from in situ and remote sensing
590 techniques during the DEMEVAP 2011 campaign at OHP, Atmospheric Meas. Tech., 6, 2777–
591 2802, https://doi.org/10.5194/amt-6-2777-2013, 2013.

592 Buck, A. L.: New Equations for Computing Vapor Pressure and Enhancement Factor, J. Appl.
593 Meteorol., 20, 1527–1532, https://doi.org/10.1175/1520-
594 0450(1981)020<1527:NEFCVP>2.0.CO;2, 1981.

595 Dai, A., Wang, J., Thorne, P. W., Parker, D. E., Haimberger, L., and Wang, X. L.: A New Approach
596 to Homogenize Daily Radiosonde Humidity Data, J. Clim., 24, 965–991,
597 https://doi.org/10.1175/2010JCLI3816.1, 2011.

598 Dirksen, R. J., Sommer, M., Immler, F. J., Hurst, D. F., Kivi, R., and Vömel, H.: Reference quality
599 upper-air measurements: GRUAN data processing for the Vaisala RS92 radiosonde,
600 Atmospheric Meas. Tech., 7, 4463–4490, https://doi.org/10.5194/amt-7-4463-2014, 2014.

601 Dirksen, R. J., Haefele, A., Vogt, F. P. A., Sommer, M., Von Rohden, C., Martucci, G., Romanens,
602 G., Felix, C., Modolo, L., Vömel, H., Simeonov, T., Oelsner, P., Edwards, david, Oakley, T.,
603 Gardiner, T., and Imran Ansari, M.: Report of WMO's 2022 Upper-Air Instrument
604 Intercomparison Campaign, 2024.

605 Dupont, J.-C., Haeffelin, M., Badosa, J., Clain, G., Raux, C., and Vignelles, D.: Characterization
606 and Corrections of Relative Humidity Measurement from Meteomodem M10 Radiosondes at
607 Midlatitude Stations, J. Atmospheric Ocean. Technol., 37, 857–871,
608 https://doi.org/10.1175/JTECH-D-18-0205.1, 2020.

609 Durre, I., Yin, X., Vose, R. S., Applequist, S., and Arnfield, J.: Enhancing the Data Coverage in
610 the Integrated Global Radiosonde Archive, J. Atmospheric Ocean. Technol., 35, 1753–1770,
611 https://doi.org/10.1175/JTECH-D-17-0223.1, 2018.

612 Fischer, L., Kiemle, C., and Craig, G. C.: Height-resolved variability of midlatitude tropospheric
613 water vapor measured by an airborne lidar, Geophys. Res. Lett., 39, 2011GL050621,
614 https://doi.org/10.1029/2011GL050621, 2012.

615 Gierens, K., Matthes, S., and Rohs, S.: How Well Can Persistent Contrails Be Predicted?,
616 Aerospace, 7, 169, https://doi.org/10.3390/aerospace7120169, 2020.

617 Hersbach, H., Bell, B., Berrisford, P., Hirahara, S., Horányi, A., Muñoz-Sabater, J., Nicolas, J.,
618 Peubey, C., Radu, R., Schepers, D., Simmons, A., Soci, C., Abdalla, S., Abellan, X., Balsamo, G.,
619 Bechtold, P., Biavati, G., Bidlot, J., Bonavita, M., De Chiara, G., Dahlgren, P., Dee, D.,
620 Diamantakis, M., Dragani, R., Flemming, J., Forbes, R., Fuentes, M., Geer, A., Haimberger, L.,
621 Healy, S., Hogan, R. J., Hólm, E., Janisková, M., Keeley, S., Laloyaux, P., Lopez, P., Lupu, C.,

https://doi.org/10.5194/egusphere-2026-482
Preprint. Discussion started: 3 March 2026

Radnoti, G., De Rosnay, P., Rozum, I., Vamborg, F., Villaume, S., and Thépaut, J.: The ERA5 global reanalysis, Q. J. R. Meteorol. Soc., 146, 1999–2049, https://doi.org/10.1002/qj.3803, 2020.

Hofer, S., Gierens, K., and Rohs, S.: How well can persistent contrails be predicted? An update, Atmospheric Chem. Phys., 24, 7911–7925, https://doi.org/10.5194/acp-24-7911-2024, 2024.

Hoshino, S., Sugidachi, T., Shimizu, K., Kobayashi, E., Fujiwara, M., and Iwabuchi, M.: Comparison of GRUAN data products for Meisei iMS-100 and Vaisala RS92 radiosondes at Tateno, Japan, Atmospheric Meas. Tech., 15, 5917–5948, https://doi.org/10.5194/amt-15-5917-2022, 2022.

Hyland, R. W. and Wexler, A.: Formulations for the thermodynamic properties of the saturated phases of H2O from 173.15 K to 473.15 K, ASHRAE Trans., 89, 500–519, 1983.

IPCC: Climate Change 2013: The Physical Science Basis. Contribution of Working Group I to the Fifth Assessment Report of the Intergovernmental Panel on Climate Change, [Stocker, T.F., D. Qin, G.-K. Plattner, M. Tignor, S.K. Allen, J. Boschung, A. Nauels, Y. Xia, V. Bex and P.M. Midgley (eds.)]. Cambridge University Press, Cambridge, United Kingdom and New York, NY, USA, 2013.

Kärcher, B.: Formation and radiative forcing of contrail cirrus, Nat. Commun., 9, 1824, https://doi.org/10.1038/s41467-018-04068-0, 2018.

Khaykin, S., Pommereau, J.-P., Korshunov, L., Yushkov, V., Nielsen, J., Larsen, N., Christensen, T., Garnier, A., Lukyanov, A., and Williams, E.: Hydration of the lower stratosphere by ice crystal geysers over land convective systems, Atmospheric Chem. Phys., 9, 2275–2287, https://doi.org/10.5194/acp-9-2275-2009, 2009.

Konjari, P., Rolf, C., Hegglin, M. I., Rohs, S., Li, Y., Zahn, A., Bönisch, H., Nedelec, P., Krämer, M., and Petzold, A.: Technical note: Water vapour climatologies in the extra-tropical upper troposphere and lower stratosphere derived from a synthesis of passenger and research aircraft measurements, Atmospheric Chem. Phys., 25, 4269–4289, https://doi.org/10.5194/acp-25-4269-2025, 2025.

Lang, T., Naumann, A. K., Stevens, B., and Buehler, S. A.: Tropical Free-Tropospheric Humidity Differences and Their Effect on the Clear-Sky Radiation Budget in Global Storm-Resolving Models, J. Adv. Model. Earth Syst., 13, e2021MS002514, https://doi.org/10.1029/2021MS002514, 2021.

Lee, D. S., Fahey, D. W., Skowron, A., Allen, M. R., Burkhardt, U., Chen, Q., Doherty, S. J., Freeman, S., Forster, P. M., Fuglestvedt, J., Gettelman, A., De León, R. R., Lim, L. L., Lund, M. T., Millar, R. J., Owen, B., Penner, J. E., Pitari, G., Prather, M. J., Sausen, R., and Wilcox, L. J.: The contribution of global aviation to anthropogenic climate forcing for 2000 to 2018, Atmos. Environ., 244, 117834, https://doi.org/10.1016/j.atmosenv.2020.117834, 2021.

McCarthy, M. P., Thorne, P. W., and Titchner, H. A.: An Analysis of Tropospheric Humidity Trends from Radiosondes, J. Clim., 22, 5820–5838, https://doi.org/10.1175/2009JCLI2879.1, 2009.

https://doi.org/10.5194/egusphere-2026-482
Preprint. Discussion started: 3 March 2026

Miloshevich, L. M., Vömel, H., Paukkunen, A., Heymsfield, A. J., and Oltmans, S. J.: Characterization and Correction of Relative Humidity Measurements from Vaisala RS80-A Radiosondes at Cold Temperatures, J. Atmospheric Ocean. Technol., 18, 135–156, https://doi.org/10.1175/1520-0426(2001)018<0135:CACORH>2.0.CO;2, 2001.

Miloshevich, L. M., Vömel, H., Whiteman, D. N., Lesht, B. M., Schmidlin, F. J., and Russo, F.: Absolute accuracy of water vapor measurements from six operational radiosonde types launched during AWEX-G and implications for AIRS validation, J. Geophys. Res. Atmospheres, 111, 2005JD006083, https://doi.org/10.1029/2005JD006083, 2006.

Nash, J., Oakley, T., Vömel, H., and Wei, L.: WMO intercomparison of high quality radiosonde systems, Yangjiang, China, 2010.

Pruppacher, H. R. and Klett, J. D.: Microphysics of clouds and precipitation, 2nd rev. and enl. ed., Kluwer Academic Publishers, Dordrecht, 1997.

Ruzmaikin, A., Aumann, H. H., and Manning, E. M.: Relative Humidity in the Troposphere with AIRS, J. Atmospheric Sci., 71, 2516–2533, https://doi.org/10.1175/JAS-D-13-0363.1, 2014.

Seidel, D. J., Berger, F. H., Diamond, H. J., Dykema, J., Goodrich, D., Immler, F., Murray, W., Peterson, T., Sisterson, D., Sommer, M., Thorne, P., Vomel, H., and Wang, J.: Reference Upper-Air Observations for Climate: Rationale, Progress, and Plans, Bull. Am. Meteorol. Soc., 90, 361–369, https://doi.org/10.1175/2008BAMS2540.1, 2009.

Shao, X., Ho, S.-P., Jing, X., Zhou, X., Chen, Y., Liu, T.-C., Zhang, B., and Dong, J.: Characterizing the tropospheric water vapor spatial variation and trend using 2007–2018 COSMIC radio occultation and ECMWF reanalysis data, Atmospheric Chem. Phys., 23, 14187–14218, https://doi.org/10.5194/acp-23-14187-2023, 2023.

Sherwood, S. C., Roca, R., Weckwerth, T. M., and Andronova, N. G.: Tropospheric water vapor, convection, and climate, Rev. Geophys., 48, RG2001, https://doi.org/10.1029/2009RG000301, 2010.

Smit, H. G. J., Rohs, S., Neis, P., Boulanger, D., Krämer, M., Wahner, A., and Petzold, A.: Technical Note: Reanalysis of upper troposphere humidity data from the MOZAIC programme for the period 1994 to 2009, Atmospheric Chem. Phys., 14, 13241–13255, https://doi.org/10.5194/acp-14-13241-2014, 2014.

Song, H.-J., Kim, S., Lee, H., and Kim, K.-H.: Climatology of Tropospheric Relative Humidity over the Korean Peninsula from Radiosonde and ECMWF Reanalysis, Atmosphere, 11, 704, https://doi.org/10.3390/atmos11070704, 2020.

Sonntag, D.: Fortschritte in der Hygrometrie, Meteorol. Z., 3, 51–66, https://doi.org/10.1127/metz/3/1994/51, 1994.

Sperber, D. and Gierens, K.: Towards a more reliable forecast of ice supersaturation: concept of a one-moment ice-cloud scheme that avoids saturation adjustment, Atmospheric Chem. Phys., 23, 15609–15627, https://doi.org/10.5194/acp-23-15609-2023, 2023.

https://doi.org/10.5194/egusphere-2026-482
Preprint. Discussion started: 3 March 2026

698 Tompkins, A. M., Gierens, K., and Rädel, G.: Ice supersaturation in the ECMWF integrated
699 forecast system, Q. J. R. Meteorol. Soc., 133, 53–63, https://doi.org/10.1002/qj.14, 2007.

700 Virman, M., Bister, M., Räisänen, J., Sinclair, V. A., and Järvinen, H.: Radiosonde comparison of
701 ERA5 and ERA-Interim reanalysis datasets over tropical oceans, Tellus Dyn. Meteorol.
702 Oceanogr., 73, 1929752, https://doi.org/10.1080/16000870.2021.1929752, 2021.

703 Vömel, H., Berger, F. H., Immler, F. J., Seidel, D. J., and Thorne, P.: The GCOS Reference Upper-
704 Air Network (GRUAN), in: EGU General Assembly Conference Abstracts, 1941, 2009.

705